



Atbara Water Current Turbine



Osama Mohammed Elmardi Suleiman ^a
Mahmoud Yassin Osman ^b

Article history:

Received: 9 January 2018

Revised: 25 April 2018

Approved: 10 May 2018

Published: 17 May 2018

Keywords

Efficiencies;

Aerofoil Sections;

The coefficient of Lift and Drag;

Flowing Rivers Water

Turbines;

Abstract

The motivation that led to the writing of the present paper is the necessity to exploit the high-velocity energy of River Nile that obtained when River Atbara meets River Nile in Atbara town which is located in River Nile State. At the junction of the two rivers high-velocity energy is gained, and therefore, a suitable energy converter is needed to utilize this abundant energy. This research paper is a continuation of a series of researches executed by the Faculty of Engineering and Technology Atbara to utilize the hydraulic energy of River Nile and try to convert it into a suitable form of energy for the general good of the simple citizens of River Nile and the Northern States. It was found that the efficiency of the energy converter (i.e. water current turbine) increases with the increase of the angle of incidence. It reaches a peak value of approximately 35.7% at 83 degrees, and then it decreases sharply with any further increase in the angle of incidence.

© Copyright 2018. The Author.

Published by POAJ in Universidad Técnica de Manabí.

This is an open-access article under the CC-BY-SA license

(<http://creativecommons.org/licenses/by-nc-sa/4.0/>)

All rights reserved.

Author correspondence:

Department of Mechanical Engineering,

Faculty of Engineering,

Kassala University, Kassala, Kassala State, Sudan

Email address: osamamm64@gmail.com

1. Introduction

The increased consumption of energy resources year after another has been threatening our globe since the inception of the industrial revolution before the three-quarters century. The invention of engines and machines has been followed by drilling the ground searching for oil and other mineral resources. This eager and crazy race of trying to possess the available forms of energy by any means, and to convert it into products and/or services for the welfare of human beings encourages the scientists and researchers to do their best in order to save the world limited resources from replenishment. The scientific research was, therefore, being directed towards finding other resources of energy which must be continuous and eternal i.e. renewable energy like solar, wind, biological, gas, underground latent heat, and water-current energy. These forms of energy can be utilized with very small or approximately no

^a Nile Valley University, (Sudan/East Africa)

^b Kassala University,(Sudan/East Africa)

running cost to solve completely or partially the energy problems in many countries throughout the world. But now the problem is the elevated initial cost of constructing the converting units which are capable of changing these raw energy sources into useful forms.

The utilization of water-current power was started in the first century, where the river's water-current was used to power under-water mill for crushing corn. The first mill was used in the fourth century in the middle-east with a horizontal shaft, and then it was developed to have a vertical shaft. At the beginning of the industrial revolution, the mill was used in Europe and the United States for the purpose of pumping water and wood cutting. The less well – known method of extracting energy from tidal and other flows is to convert the kinetic or velocity energy of moving water directly to the mechanical shaft without otherwise interrupting the natural flow in a manner similar to a wind turbine. This idea is not completely new as it has been investigated by Reading University in the U.K. in 1979 [1], by Davis in Canada [2] and by Hilton in Australia at about the same period [3]. It was in use in Africa on a small scale in the early 1980s to extract energy from river currents [1]. But the idea of using current flow on a large scale is new. Even as recently as 1991 a complete book on tidal energy made no mention of the concept [4]. It is only now that this concept is being explored for larger scale use [2], [5], [6], [7], [8], [9], and [10].

Direct conversion of kinetic energy by a turbine in open flow harnesses less of the total available energy in a tidal flow in an estuary that could be extracted by damming the whole estuary. However, direct conversion has several advantages:

- a) The capital cost of civil works is eliminated.
- b) Disruption to ecosystems and boating traffic is minimized.
- c) Ocean currents, wind-induced currents, and river flows, as well as tidal flows, can be used.

Here in Sudan, all the above-mentioned types of renewable energy are widely and abundantly found, but the appropriate technology of exploiting them has not yet been introduced.

The natural power of a running river or a stream has been of interest for electricity production for many years. The technology of small-scale hydropower is diverse, and different concepts have been developed and tried out [11] – [17], i.e. water current turbines with a unit power output of about 0.5–5 kw. These turbines are supposed to be used for domestic electricity applications such as lighting, battery charging, and small refrigerators and also for small pumping units. The units are small, cheap and often owned, installed and used by a single family.

Water current turbines have received a growing interest in many parts of the globe. Two main areas where these turbines can be used for pumping and/or power generation purposes are tidal currents and river streams. This book will focus on water current turbines for river applications. These turbines generate power from the kinetic energy of a flowing stream of water without the use of a dam. Water current turbines can be installed in any flow with a velocity greater than 0.5m/s [18], [19]. Because of low investment costs and maintenance fees, this technology is cost-effective in comparison to other technologies. This kind of small-scale hydropower is considered environmentally friendly, meaning that there are no toxic emissions as that exhausted from diesel engines. Small-scale water current turbines can be a solution for pumping purposes and power supply in remote areas [20].

The kinetic energy of water-currents of the river is a reliable energy source for operating mills, pumps, electrical generators etc... A current speed of (1 m/s) represents an energy flux of 500 watts per (m²) of river cross-section. Attempts to utilize this energy for pumping purposes were initiated in 1975 at Mechanical Engineering College Atbara (MECA) through students' final year project. The idea of this project was to design and create experimental data of a piston pump driven by a floating water wheel. After several attempts during the last twenty years, a successful approach has been reached, where a completely submerged three- blades turbine driving ordinary centrifugal pump through a speed increasing transmission is used, which is known afterward as water - current turbine.

The water current turbine which was designed and constructed in the Faculty of Engineering and Technology, Nile Valley University - Atbara is an energy converter, used to convert the kinetic energy of water currents into mechanical energy, which is in turn used to drive a centrifugal pump for irrigation purposes. This unit is composed of a rotor with three blades coupled to a shaft which transmits power to a centrifugal pump through a simple transmission system "pulleys and belts" as shown in figure 8. Water is pumped from the river to the irrigation canal on the river bank through a rigid pipeline which also acts as an access walkway to the machine. All this arrangement is carried on buoyant barrels closed at both ends and connected by steel frame or bed. This unit develops about 1000 watts with an overall efficiency of 24 percent and costs about 6 million Sudanese pounds (i.e. fifteen thousand pounds in today's price), the initial cost of the construction of this unit is relatively high compared with Lister diesel engine for the same output power. This induces the idea of this project in order to improve the ratio of power

developed per initial cost through modifying the previous design of the whole system using the following procedures:

There are two areas which can be investigated to comply with the modified objectives.

- a) To establish data of performance concerning Atbara water-current turbine for the first time i.e. to determine speed and torque for different angles of attack for the two proposed types of aerofoils, the straight – cambered and the cambered – cambered aerofoils.
- b) To propose some changes in Atbara water-current turbine in order to improve the existing designs.

Aerofoil Definition

An aerofoil is a streamlined body designed to produce lift with minimum drag. In a streamlined body, immersed in a flowing fluid, separation is delayed till near the rear. This will decrease the drag on the streamlined body to a minimum value. The drag in a streamlined body can be as low as 1/15 of that on a cylinder of the same thickness.

The most important feature is the slowly tapering tail. This is the reason why streamlining of a railway engine with a train behind it makes an only marginal difference. On the other hand, it is essential to their performance that the wings and fuselage of an airplane and the parts of a submarine should have streamlined profiles. It is also apparent that the shapes are shown in figures 1 and 2 resemble the shape of many marine creatures i.e. fishes, dolphins etc... (Refer to references [21] – [33]).

2. Research Methods

Figure 1 shows a typical aerofoil section and some of the terms relating to it. These terms are as follows:

Leading Edge: It is the edge which faces the direction of flow firstly and sometimes referred to as a nose.

Trailing Edge: It is the far edge of the rear edge of an aerofoil.

Chord: It is the distance between the leading edge and the trailing edge points.

Chord Line: It is the straight line drawn to connect the two edges together.

Camber Line: It is the line connecting the two edges so that it should pass through the centroid of an aerofoil.

The angle of Incidence: It is the angle at which the chord line of an aerofoil makes with the the direction of flow and sometimes referred to as the angle of attack.

a) Geometrical Parameters

The characteristics of an aerofoil section are largely determined by some geometrical parameters. These parameters are:

(t/c) Ratio: It is the ratio between the maximum thickness (t) and the chord line (C).

(x/c) Ratio: It is the ratio between the position of the maximum thickness of the nose and the chord length.

Percentage Camber: It is the ratio between the maximum camber and the chord length (as a percentage).

Percentage Nose Radius: It is the nose radius of curvature as a percentage of the chord length.

Trailing Edge Angle: It is the angle between the upper and lower surfaces at the trailing edge.

b) Aerofoil Types

Aerofoils are generally classified into two types; symmetric and asymmetric aerofoils.

- (1) **Symmetric Aerofoils:** The main feature in this type of aerofoils is that the camber line coincides with the chord line as shown in figure 2. These aerofoils are rarely used in practice since higher values of lift and lower values of drag can still be obtained by other types of aerofoils.
- (2) **Asymmetric Aerofoils:** The ratio between lift and drag (L/D) can be improved by using asymmetric aerofoils. In these aerofoils the camber line doesn't coincide with the chord line as shown in figure 1, the simplest form of asymmetric aerofoils is called cambered aerofoils in which the camber line is made into a circular arc. In cambered aerofoils, both faces can be made curved in one direction or the top face curved while the bottom face is straight as shown in figure 3 {(a) and (b)}.

c) Generation of Lift and Drag

If an aerofoil is placed in a stream of a flowing fluid, the streamlines around the aerofoil will be deflected resulting in a decrease in pressure on the upper surface and an increase in pressure on the lower surface. Due to this difference in pressure a force is generated which may be resolved into two components: a component parallel to the direction of flow giving the drag force (D), and a second component normal to the mainstream giving the lift force (L) as shown in figure 1, both lift and drag forces are substituted in terms of the maximum dynamic force (\hat{F}) which is given by the formula:

$$\hat{F} = \frac{1}{2} \rho u_0^2 A \quad (\text{N}) \quad (1)$$

Where; ρ = water density in (kg/m^3).

u_0 = relative velocity between the flowing fluid and the body in (m/s).

A = projected area on the chord line in (m^2).

The lift force is:

$$L = \frac{1}{2} C_L \rho u_0^2 A \quad (\text{N}) \quad (2)$$

The drag force is:

$$D = \frac{1}{2} C_D \rho u_0^2 A \quad (\text{N}) \quad (3)$$

Where; C_L = Coefficient of lift.

C_D = coefficient of drag.

The ratio (L/D) or $\{C_L/C_D\}$ is very important and it depends on the angle of incidence (α) and other geometrical parameters.

The best angle of incidence is one which gives the maximum value of $\{C_L/C_D\}$. With the increase of angle of incidence from zero, the suction (negative pressure) increases over the upper surface, particularly towards the leading edge and with it the lift increases. However, at a sufficiently high incidence, the adverse pressure gradient following the peak approaches a value for which boundary layer separation develops. With further increase of incidence, the flow separation rapidly spreads over the upper surface, and the peak suction falls. In this case over the region of the separated flow, the pressure becomes more nearly constant over the surface whilst the trailing edge pressure and the lift fall. The wing is then said to be stalled.

The performance of any aerofoil blade can be drawn in a graph showing the variations of lift coefficient (C_L) and drag coefficient (C_D) with the incidence angle (α). Figure 4 shows atypical variations of the coefficient of lift (C_L) and coefficient of drag (C_D) with angles of incidence (α).

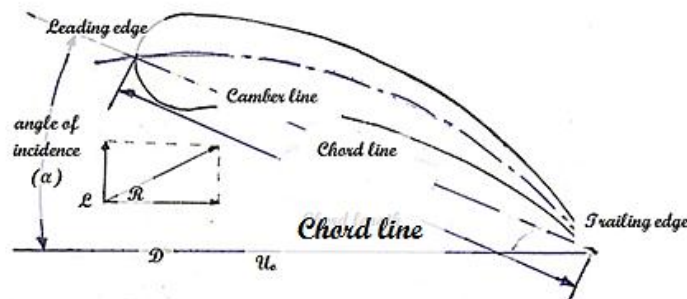


Figure 1. Asymmetric Aerofoil

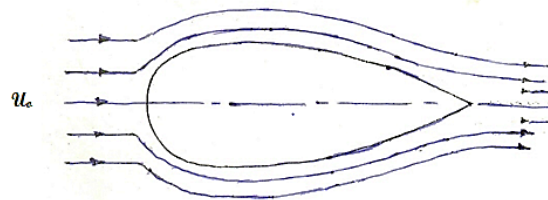


Figure 2. Symmetric Aerofoil

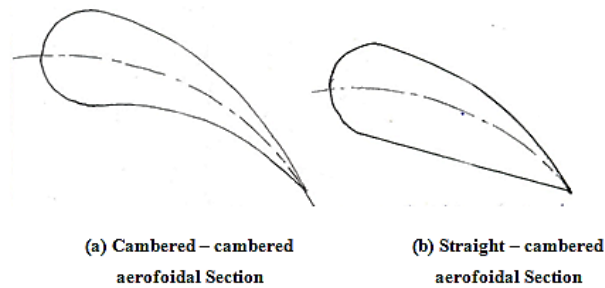
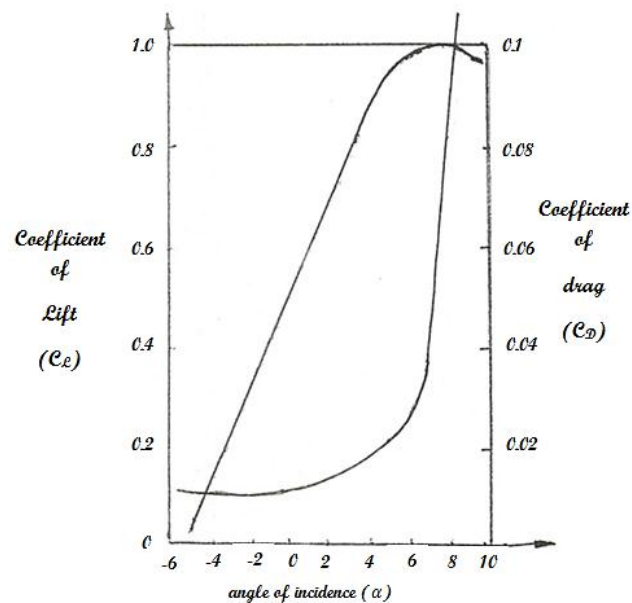


Figure 3. Two Types of Aerofoil Section Profiles

Figure 4. Variation of C_L and C_D with α for A typical Aerofoil

d) Model Design and Testing Procedures

- (1) Model Design: Two types of asymmetric cambered aerofoils blades were selected for testing and compared for efficiency and performance. One type is geometrically similar to that one used in the existing water-current turbine belonging to the Faculty of Engineering and Technology-Atbara, (i.e. straight –cambered aerofoil) and the other type is of different geometric shape (i.e. cambered – cambered aerofoil), which was expected to be to some extent more efficient than the first one. The first type has almost an upper curved surface and a straight lower surface, while the second type has curved profiles on both surfaces.

The Straight – Cambered Aerofoil: The model is made to a scale of 4:5 of the full size turbine (i.e. Atbara

water current turbine). This aerofoil has the following geometrical parameters:

Chord (c) = 160 mm
 Maximum thickness (t) = 40 mm
 Span (s) = 400 mm
 (t/c) Ratio = 25%
 (x/c) Ratio = 18%
 Position of maximum thickness from the nose (x) = 29 mm.
 Percentage camber = 4%
 Percentage nose radius = 12.5%
 Trailing edge angle = 25 degrees

Figure 5 shows the straight – cambered aerofoil model drawn in full-size dimensions.

The Cambered – Cambered Aerofoil: The model is made of the same dimensions as that of the straight – cambered aerofoil. This aerofoil has the following geometrical parameters:

Chord (c) = 160 mm
 Maximum thickness (t) = 36 mm
 Span (s) = 400 mm
 (t/c) Ratio = 22.5%
 (x/c) Ratio = 12.5%
 The position of maximum thickness from the nose (x) = 20 mm.
 Percentage camber = 8.5%
 Percentage nose radius = 12.5%
 Trailing edge angle = 20 degrees

This aerofoil which is desired to be compared with the straight-cambered aerofoil is shown full-size in figure 6.

Blades Manufacturing: Two sets of blades were made of plywood. Each set includes three similar blades; the first set is of a section profile of a straight-cambered aerofoil while the second set is of a cambered – cambered aerofoil. The tip of each blade was rounded so as to decrease the trailing vortices. All blades were painted with a metallic paint where several layers of paint were made in order to prevent water penetration. A piece of mild steel strip with welded nut was bolted to each blade for the purpose of securing the blade to the screw of the boss. A pointer was fixed to the lower end of each blade at the leading edge (i.e. nose) for the purpose of adjusting the angle of incidence, and a set of three protractors is fixed to the boss under the blades so as to adjust the required angle of incidence.

Design and Manufacturing of Chassis and Shaft:

The Chassis: The chassis consists of two parts: one part has two bearing brackets 40mm diameter for holding the shaft while the other part is used for fixing the whole arrangement to the chassis of the already existing water – current turbine at Atbara River-Nile which is shown in the figure . The former part is inclined at 38° to the horizontal (i.e. similar to that already existing one), so as to allow the rotor to be completely immersed in water. A 36mm mild steel angle plate is used for manufacturing the whole chassis. Welding, riveting and bolting techniques are used for joining the various pieces of the chassis. Figure 7 shows the basic parts of water current turbine holding mechanism.

The Shaft: It is a hollow shaft 1.2m long and a 30mm diameter made of mild steel. It has a boss made of a circular mild steel disc 100mm diameter and 10mm thickness. This boss is welded rigidly to the shaft and has 3 equispaced screws (M10) for holding the blades. At each screw, a protractor is fixed by means of a nut and washers. The other end of the shaft is closed by welding a mild steel disc plate on it. The purpose of the protractors and the pointers is to measure the different angles of incidence required during the test.

The Prony Brake: A Prony brake is made of mild steel strip 25mm wide and 3mm thick. It has an arm length of 190mm measured from the center of rotation of the shaft. A spring balance of the range (0–100N) is used in conjunction with the Prony brake to form a torque measuring system. The torque needed to be measured is that transmitted by the shaft. A vertical holder fixed to the inclined part of the chassis is used for holding the spring balance.

A stopwatch is used for measuring the rotational speed of the shaft. This method is done by counting the number of revolutions of the shaft in one minute.

A current flow meter type B FM 001 English made is used for measuring the current velocity at equal intervals during the test, where several readings are taken and the average value is calculated.

(2) **Testing Procedures:** The procedures which are followed at any reading can be summarized in the following

Suleiman, O., & Osman, M. (2018). Atbara water current turbine. International Journal Of Engineering & Computer Science (IJECS), 1(1), 30-46. doi:10.31295/ecs.v1n1.21

points:

- a. Raising the immersed rotor outside the water after breaking the shaft with the Prony brake device.
- b. Using spanner for adjusting the angle of incidence of the three blades in turn as required.
- c. Lowering the rotor so as to be completely immersed in water and fixing it at this position.
- d. Releasing the Prony brake to liberate the shaft and allow it to rotate about 1 minute approximately before taking the new reading.
- e. Using a stopwatch and a tachometer to count the number of revolutions of the shaft during one minute. This will represent the shaft speed in rev/min.
- f. Applying the Prony brake to the shaft until it is completely stopped, and then the spring-balance reading is recorded.
- g. The speed of rotation and the spring balance readings are taken three times per each setting of the angle of incidence, and then the average values are registered.
- h. The reading of the current velocity is taken by the current flow-meter at every setting and then a mean value is recorded.
- i. Repeating the above procedures for each setting of the angle of incidence.

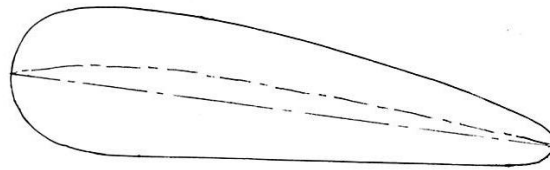


Figure 5. The Straight – Cambered Aerofoil Drawn in Full – Size Dimensions



Figure 6. The Cambered – Cambered Aerofoil Drawn in Full – Size Dimensions

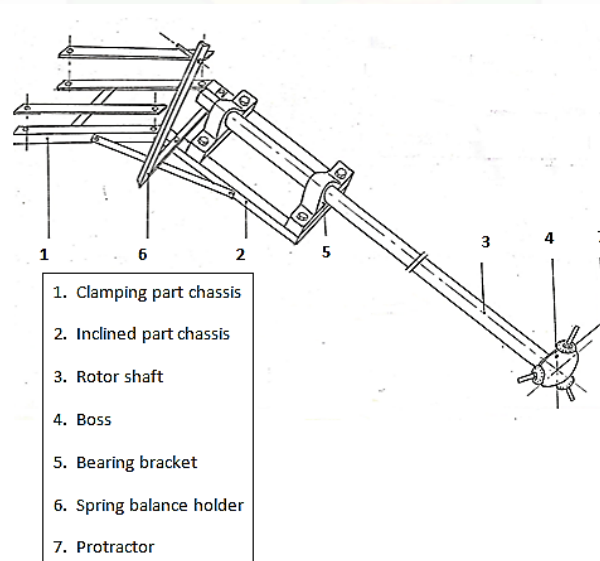


Figure 7. The Holding Mechanism of the Water – Current Turbine Model

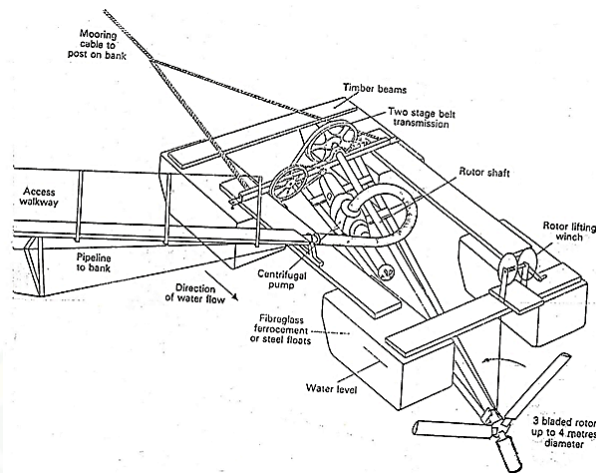


Figure 8. The Full – Size Water Current Turbine
(Atbara Water Current Turbine)

3. Results and Analysis

Readings: Tables 1 and 2 show the readings obtained from testing the straight-cambered aerofoil and cambered – cambered aerofoil respectively.

A sample of Calculations: The test readings which are taken from table 1 are as follows:

$$\begin{aligned}\alpha &= 60^\circ \\ u_o &= 1.075 \text{ m/s} \\ N &= 38 \text{ rev/min} \\ \ell &= 10^3 \text{ kg/m}^3 \\ F &= 44\text{N} \\ c &= 0.16 \text{ m} \\ r &= 0.19 \text{ m}\end{aligned}$$

Where;

$$\begin{aligned}\alpha &= \text{angle of incidence} \\ u_o &= \text{average water current speed} \\ N &= \text{shaft speed} \\ \ell &= \text{density of water} \\ F &= \text{brake force} \\ c &= \text{chord length} \\ r &= \text{arm length of the Prony brake}\end{aligned}$$

From table 1 as an example and at an angle of incidence equivalent to 60° the shaft speed and the brake force are equivalent to 38 RPM and 44 N respectively. Then, the following quantities can be calculated as follows:

$$\begin{aligned}\text{Torque, } T &= F \cdot r \\ &= 44 \times 0.19 \\ &= 8.36 \text{ N.m} \\ \text{Output power, } P_o &= \frac{2\pi TN}{60} \\ &= \frac{2\pi \times 8.36 \times 38}{60} \\ &= 33.27 \text{ W} \\ \text{Input power, } P_i &= \frac{1}{2} \ell u_o^3 A \cos 38\end{aligned}$$

$$\begin{aligned}
 &= \frac{1}{2} \times 10^3 (1.075)^3 \frac{\pi}{4} [1^2 - 0.2^2] \cos 38 \\
 &= 370 \text{ W (constant value)} \\
 \text{Efficiency, } \eta &= (P_o/P_i) 100\% \\
 &= \frac{33.27}{370} \times 100\% \\
 &= 9.00\%
 \end{aligned}$$

$$\begin{aligned}
 \text{Maximum dynamic force, } \bar{F}, \text{ per unit span} \\
 &= \frac{1}{2} \times \ell u^2 c \\
 &= \frac{1}{2} \times 10^3 (1.075)^2 \times 0.16 \\
 &= 92 \text{ N (constant value)}
 \end{aligned}$$

Lift force, $L = T/R$

Lift force per unit span, $L' = T/ SR$

Where;

$R =$ mean radius of blade circle $= 0.3 \text{ m}$

$S =$ span $= 0.4 \text{ m}$

$L' = 8.36 / (0.4 \times 0.3)$
 $= 70 \text{ N}$

$$\begin{aligned}
 \text{Coefficient of lift, } C_L &= \frac{L'}{\bar{F}} \\
 &= \frac{70}{92} \\
 &= 0.76
 \end{aligned}$$

Results: Tables 3 and 4 show the results calculated from the readings of the straight-cambered aerofoil and the cambered – cambered aerofoil respectively.

Comments on Graphs and Results Analysis:

1) Straight – Cambered Aerofoil:

Graph of Efficiency against Angle of Incidence: Figure 9 and table 3 show the variation of the efficiency of the turbine model with respect to the different angle of incidence ranging between 0 and 96°. It shows that the efficiency increases with the increase of the angle of incidence where it reaches a peak value of 35.7% at 83 degrees, and then it decreases sharply with any additional increase in the angle of incidence.

Graph of Coefficient of Lift against Angle of Incidence: Figure 10 and table 3 show the variation of coefficient of lift with various angles of incidence ranging from zero to 96°. At an angle of incidence of zero, the coefficient of lift is zero. The coefficient of lift increases with the increase of the angle of incidence where it reaches a maximum value of 1.45 at 83 degrees and then decreases sharply with the increase in the angle of incidence.

2) Cambered – Cambered Aerofoil:

Graph of Efficiency against Angle of Incidence: Figure 11 and table 4 show the variation of the efficiency of the model with different angles of incidence fluctuating between 0 and 96°. The efficiency increases with the increase of the angle of incidence till it reaches a maximum value of 23.6 percent at an angle of 78 degrees, and then decreases sharply until it reaches a zero value at an angle of incidence equivalent to 85 degrees, and then it increases sharply to another peak value of 21 percent at 95 degrees.

Graph of Coefficient of Lift against Angle of Incidence: Figure 12 and table 4 show the variation of coefficient of lift with various angles of incidence fluctuating between 0 and 96°. The coefficient of lift is zero at (- 6) degrees angle of incidence, and at zero angles of incidence, the coefficient of lift is 0.9. The maximum value of the coefficient of lift is 1.13 and occurs at two incidence angles, one at 78 degrees (positive value) and the other at 94 degrees (negative value). The negative coefficient of the lift means opposite direction of rotation.

Table 1
Readings of the Straight – Cambered Aerofoil

The angle of Incidence (α) (degrees)	Speed (N) (RPM)	Spring -balance Reading (F) (N)
0	0.0	0
2	1.5	4
4	2.5	9
5	2.5	12
6	3.0	15
7	3.0	17
8	3.5	18
9	4.0	19
10	4.0	20
15	6.0	22
20	8.0	25
30	12.0	29
40	19.0	34
50	26.0	38
60	38.0	44
70	52.0	48
80	56.0	53
81	60.0	59
82	65.0	63
83	78.0	85
84	74.0	80
86	70.0	70
88	64.0	50
90	42.0	32
92	36.0	26
94	30.0	23
96	20.0	17

Table 2
Readings of the Cambered – Cambered Aerofoil

The angle of Incidence (α) (degrees)	Speed (N) (RPM)	Spring -balance Reading (F) (N)
-6	0.0	0.0
-4	2	12
-2	4	38
0	5	52
2	5	48
4	6	45
5	6	43
6	7	40
7	8	38
8	8	35
9	10	36
10	11	38
15	12	40
20	14	42

30	16	46
40	25	52
50	32	55
60	46	60
70	58	65
80	55	62
81	52	56
82	50	52
83	46	44
84	40	30
86	-28	36
88	-44	54
90	-51	58
92	-54	62
94	-56	66
96	-58	60

Table 3
Calculated Results of the Straight – Cambered Aerofoil

(α) (deg.)	Torque (Nm)	Output Power (W)	Efficiency (%)	Lift / unit span (N/m)	Coefficient of Lift (C_L)
0	0.00	0.00	0.00	0.00	0.00
2	0.76	0.12	0.04	6.34	0.07
4	1.71	0.45	0.13	14.25	0.15
5	2.28	0.60	0.17	19.00	0.21
6	2.85	0.90	0.25	23.76	0.26
7	3.23	1.02	0.28	26.92	0.29
8	3.42	1.26	0.34	28.50	0.31
9	3.61	1.52	0.42	30.08	0.33
10	3.80	1.60	0.44	31.66	0.34
15	4.18	2.63	0.72	34.84	0.38
20	4.75	3.98	1.08	39.60	0.43
30	5.51	6.93	1.90	46.00	0.49
40	6.46	12.86	3.48	54.00	0.59
50	7.22	19.66	5.32	60.16	0.65
60	8.36	33.27	9.00	70.00	0.75
70	9.12	49.70	13.43	76.00	0.82
80	10.07	59.06	16.00	83.92	0.91
81	11.21	70.44	19.04	93.42	1.01
82	11.97	81.48	22.02	99.76	1.06
83	16.15	132.00	35.68	134.60	1.45
84	15.20	117.79	31.84	126.66	1.37
86	13.30	97.50	26.35	110.84	1.20
88	9.50	63.67	17.21	79.16	0.86
90	6.08	26.75	7.23	50.66	0.55
92	4.94	18.62	5.03	41.16	0.45
94	4.37	13.73	3.71	36.42	0.39
96	3.23	6.80	1.83	10.77	0.12

Table 4
Calculated Results of the Cambered – Cambered Aerofoil

(α) (deg.)	Torque (Nm)	Output Power (W)	Efficiency (%)	Lift /unit span (N/m)	Coefficient of Lift (C_L)
-6	0.00	0.00	0.00	0.00	0.00
-4	2.30	0.48	0.13	19.00	0.21
-2	7.20	3.04	0.82	6.00	0.65
0	9.90	5.20	1.41	82.50	0.90
2	9.10	4.78	1.30	76.00	0.92
4	8.60	5.37	1.45	72.00	0.78
5	8.20	5.13	1.39	68.50	0.74
6	7.60	5.58	1.51	63.50	0.69
7	7.20	6.06	1.64	60.00	0.65
8	6.70	5.58	1.51	56.00	0.60
9	6.80	7.17	1.94	56.50	0.61
10	7.20	8.33	2.25	60.00	0.65
15	7.60	9.55	2.58	63.50	0.69
20	8.00	11.70	3.16	66.50	0.72
30	8.70	14.64	4.00	72.50	0.80
40	9.900	25.90	7.00	82.50	0.90
50	10.45	35.02	9.47	87.00	0.94
60	11.40	54.92	14.85	95.00	1.03
70	12.35	75.01	20.28	103.00	1.12
80	11.78	67.85	18.34	98.00	1.06
81	10.64	58.00	15.68	89.00	0.96
82	9.90	51.73	14.00	82.50	0.90
83	8.36	40.27	10.90	70.00	0.76
84	5.70	23.90	6.46	47.50	0.52
86	-6.84	20.06	5.42	-57.00	-0.61
88	-10.26	47.27	12.78	-85.50	-0.92
90	-11.0-02	58.90	15.92	-92.00	-1.00
92	-11.78	66.61	18.00	-98.00	-1.06
94	-12.54	73.54	19.88	-104.50	-1.13
96	-11.40	69.24	18.71	-95.00	-1.02

Note: Negative Sign means Opposite Direction

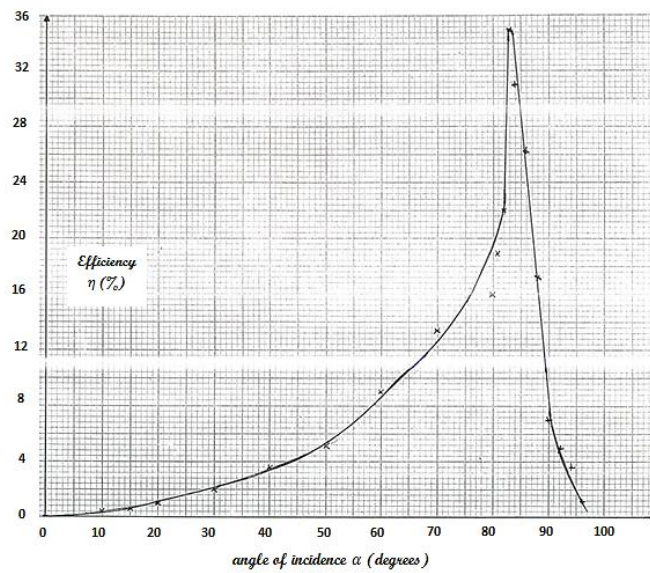


Figure 9. Efficiency against Angle of Incidence of Straight – Cambered Aerofoil

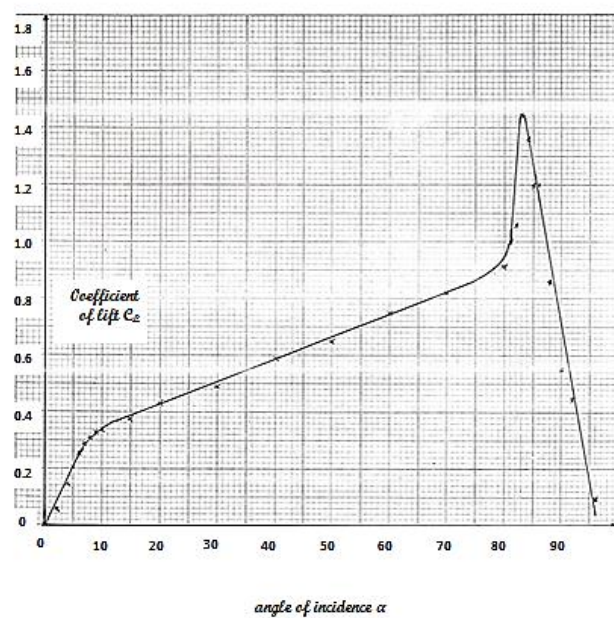


Figure 10. The coefficient of Lift against Angle of Incidence of Straight – Cambered Aerofoil

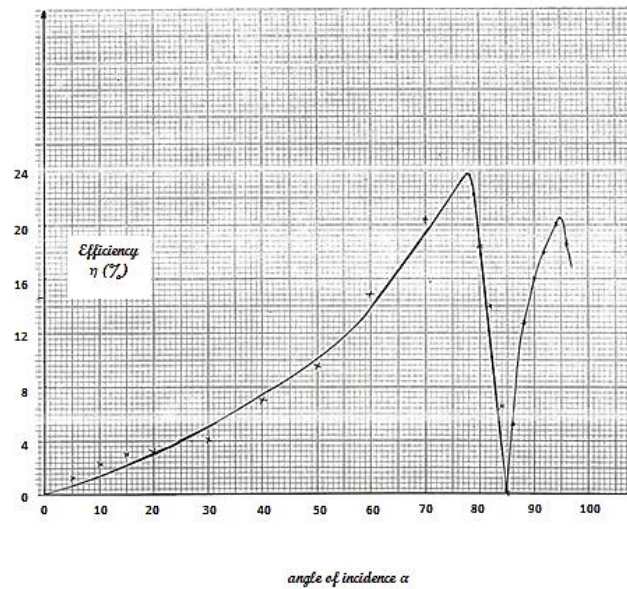


Figure 11. Efficiency against Angle of Incidence of Cambered – Cambered Aerofoil

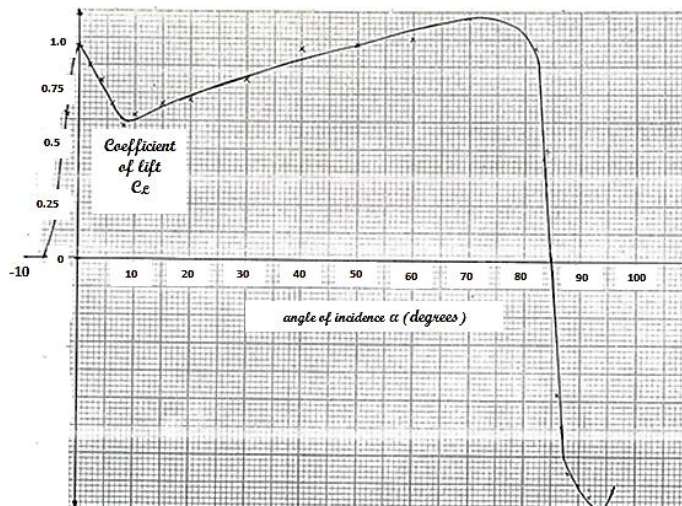


Figure 12 Coefficient of Lift against Angle of Incidence of Cambered – Cambered Aerofoil

4. Conclusion

The common factor in all rotodynamic machines is that the fluid is fed to the runner or rotating element continuously in such a way that it has a tangential velocity component (or velocity of whirl) about the axis of the shaft as it enters the runner and emerges radially or axially having lost its tangential momentum and exerted a torque on the runner in the process.

In the water-current turbine, the hydraulic energy of the fluid supplied to the machine is converted by three or more blades of aerofoil section profile into kinetic energy, and this happens because of the high difference in

pressure created due to the shape and the setting of a certain angle of attack. This action produces a force on the shaft and a torque on the blade.

It is clear from the readings taken and the corresponding graphs illustrated in chapter four, that the straight-cambered aerofoil blades give the maximum power (i.e. the product of torque and angular velocity), and this the experimental result obtained has rejected the hypothesis that the curved-cambered aerofoil would have given us the best results concerning the maximum power output, and this happens because the separation point moves extremely forward which helps the adverse pressure to build up. The hypothesis is based on the fact that curved surfaces will give high change in momentum according to its profile, but although these results are of trivial benefit in this junction, it creates opportunities for applications other than water-current turbine used for irrigation purposes. The extremely higher torques with lower speeds which have been obtained from the curved – cambered aerofoil can be of great usefulness in other engineering applications that need higher torques (for example grain mills, etc.).

From the results obtained, it is clear that the straight-cambered aerofoil gives the best results concerning the torque and speed.

The water-current turbine machine made in the Faculty of Engineering and Technology- Atbara needs some modifications in its design and consequently the manufacture of some major parts.

It is noticed that the type of transmission used is the one which works with a flat belt and pulley system. It has the advantage of less costly, light in weight and easily manufactured and also it is durable and non-corrosive (the pulley is made of aluminium alloy), but it has relatively fair efficiency of transmission (i.e. not more than 75%) in comparison to gear transmission system which has a higher efficiency of 98%. Therefore, it is recommended to use gear transmission system with the necessary anti-corrosion protection needed. Also, another advantage of the gearing transmission system is that there is a possibility of increasing or decreasing the speed through several stages without a remarkable drop in the overall efficiency.

It is also recommended that a compact design of the complete arrangement is required so as to lessen the machine size and consequently the working area. This could be attained by using a vertical shaft instead of a horizontal shaft or an inclined shaft. Consequently, testing of maximum power and efficiency may be carried out on aerofoil blades in the vertical positions which are expected to be greater than that of the inclined shaft. It is also recommended to study the effect of the thickness of the aerofoil section, the span length and chord length to the maximum power output and the overall efficiency of the system. Also, the effect of increasing and decreasing the number of blades must be studied.

Conflict of interest statement and funding sources

The author declared that he has no competing interest. The study was financed by personal funding.

Statement of authorship

The author has a responsibility for the conception and design of the study. The author has approved the final article.

Acknowledgments


The authors would like to acknowledge with deep thanks and profound gratitude Mr. Osama Mahmoud of Daniya Center for Publishing and Printing Services, Atbara, who spent many hours in editing, re-editing of the manuscript in compliance with the standard format of International Journal of Engineering & Computer Science.

References

1. Garman, P. (1986). Water current turbines. *a field worker's guide, II publications, London, 2*.
2. Khayal, O. M. E. S., & Osman, M. Y. Atbara Water Current Turbine.
3. Hilton, D. J. (1980). A vertical axis water turbine for extracting energy from rivers and tidal currents. In *First International Conference on Technology for Development 1980: Preprints of Papers* (p. 138). Institution of Engineers, Australia.
4. Baker, A. C. (1991). Tidal Power, Peter Peregrinus Ltd. *London, United Kingdom*.
5. Pearce, F. (1998). Catching the tide. *new scientist, 158(2139)*, 38-41.
6. Fraenkel, P. L., Clutterbuck, P., Stjernstrom, B., & Bard, J. (1998, September). SEAFLOW: preparing for the world's first pilot project for the exploitation of marine currents at a commercial scale. In *Proceedings of Third European Wave Energy Conference, Patras*.
7. Fraenkel, P. (1999). Tidal currents: a major new source of energy for the millennium. *Sustainable Developments International, 107-112*.
8. Fraenkel, P. L. Marine currents: a promising large clean energy source. In *Proc. I. Mech Eng Conf. "Power Generation by Renewables"*.
9. Fraenkel, P. L. (2002). Power from marine currents. *Proceedings of the Institution of Mechanical Engineers, Part A: Journal of Power and Energy, 216(1)*, 1-14.
10. Cairo, D. (2001). Department of Aeronautical Engineering, University of Naples, Pers.
11. Husain, Z., Mohd. Zulkifly Abdullah, & Alimuddin, Z. (2008). *Basic fluid mechanics and hydraulic machines*. Hyderabad, India: BS publications.
12. Gorla, R. S., & Khan, A. A. (2003). *Turbomachinery: design and theory*. CRC Press.
13. Massey, B. S., & Ward-Smith, J. (1998). *Mechanics of fluids*(Vol. 1). Crc Press.
14. Khayal, O. M. E. S., & Osman, M. Y. Experimental Research Work on Atbara Water Current Turbine in Sudan.
15. Elger, D. F., & Roberson, J. A. (2016). *Engineering fluid mechanics* (pp. 170-185). Hoboken (NJ): Wiley.
16. Douglas, J. F., & Matthews, R. D. (1996). *Solving problems in fluid mechanics*. New York: Longman.
17. Douglas, J. F., & Matthews, R. D. (1996). *Solving problems in fluid mechanics*. New York: Longman.
18. Sornes, K. (2010). Small-scale water current turbines for river applications. *Zero Emission Resource Organisation (ZERO)*.
19. Energy, T., Lane, P., & Thropton, N. N. 7HU, United Kingdom, January 2010.
20. Suleiman, O. M. E. Further Experimental Research Work on Water Current Turbines (Case Study on Atbara Water Current Turbine).
21. Daniel, I. M., Ishai, O., Daniel, I. M., & Daniel, I. (1994). *Engineering mechanics of composite materials* (Vol. 3, pp. 256-256). New York: Oxford university press.
22. Bachelor, G. K. An Introduction to Fluid Dynamics,(1967).
23. Duncan, W. J. A. S. (1978). Thom, and AD Young, 'Mechanics of fluids'.
24. Fox, R. W., & McDonald, A. T. (1994). Introduction to Fluid Mechanics, John Wiley&Sons. Inc., New York.
25. Hughes, W. F., & Brighton, J. A. (1967). *Fluid dynamics:[includes 100 solved problems]*. McGraw-Hill.
26. Iams, J. D., Goldenberg, R. L., Meis, P. J., Mercer, B. M., Moawad, A., Das, A., ... & Roberts, J. M. (1996). The length of the cervix and the risk of spontaneous premature delivery. *New England Journal of Medicine, 334(9)*, 567-573.
27. Massey, B. S., & Ward-Smith, J. (1998). *Mechanics of fluids*(Vol. 1). Crc Press.
28. Kay, J. M., & Nedderman, R. M. (1974). *An Introduction to Fluid Mechanics and Heat Transfer: with applications in chemical and mechanical process engineering*. CUP Archive.
29. Schlichting, H., Gersten, K., Krause, E., Oertel, H., & Mayes, K. (1955). *Boundary-layer theory* (Vol. 7). New York: McGraw-hill.
30. Webber, N. B. (2014). *Fluid Mechanics for Civil Engineers: SI edition*. CRC Press.
31. Streeter, V. L., Wylie, E. B., & Bedford, K. W. (1998). Fluid Mechanics, „McGraw-Hill. New York.
32. Kline, S. J. (2012). *Similitude and approximation theory*. Springer Science & Business Media.
- Suleiman, O. M. E. Further Experimental Research Work on Water Current Turbines.
33. Bento, A. C. (2018). Internet of Things: An Experiment with Residential Automation for Robotics Classes. *International Research Journal of Management, IT and Social Sciences (IRJMIS), 5(2)*, 113-119.

34. Jain, P., Jain, A., Singhai, R., & Jain, S. (2017). Effect of Biodegradation and Non Degradable Substances in Environment. *International Journal of Life Sciences (IJLS)*, 1(1), 58-64.
35. Singh, D. (2017). Leaf Phenology of Cassia Sieberiana L. in KSUSTA Campus of Kebbi State, Nigeria. *International Journal of Life Sciences (IJLS)*, 1(1), 1-8.

Biography of Author

	<p>Osama Mohammed Elmardi Suleiman Khayal was born in Atbara, Sudan in 1966. He received his diploma degree in mechanical engineering from Mechanical Engineering College, Atbara, Sudan in 1990. He also received a bachelor degree in mechanical engineering from Sudan University of Science and Technology – Faculty of Engineering in 1998, and a master degree in solid mechanics from Nile Valley University (Atbara, Sudan) in 2003. He contributed in teaching some subjects in other universities such as Red Sea University (Port Sudan, Sudan), Kordofan University (Obayied, Sudan), Sudan University of Science and Technology (Khartoum, Sudan) and Blue Nile University (Damazin, Sudan). In addition, he supervised more than hundred and fifty under graduate studies in diploma and B.Sc. levels and about fifteen master theses. He is currently an assistant professor in department of mechanical engineering, Faculty of Engineering and Technology, Nile Valley University. His research interest and favorite subjects include structural mechanics, applied mechanics, control engineering and instrumentation, computer aided design, design of mechanical elements, fluid mechanics and dynamics, heat and mass transfer and hydraulic machinery. He also works as a consultant and technical manager of Al – Kamali workshops group for small industries in Atbara old and new industrial areas.</p> <p><i>Email: osamamm64@gmail.com</i></p>
---	---